Supporting Information for

One novel 3-D chiral polyoxovanadate architecture based on breaking high symmetry of spherical $[V_{15}O_{36}Cl]^{8-}$ cluster

Jian Zhou,* Xing Liu, Feilong Hu, Rong Chen, Huahong Zou, Wensheng Fu, Guoming Liang and Yi Chen

General Remarks

All analytical grade chemicals were obtained commercially and used without further purification. Elemental analyses (C, H, and N) were performed using a PE2400 II elemental analyzer. FT-IR spectra were recorded with a Nicolet Magna-IR 550 spectrometer in dry KBr disks in the 4000-400 cm^{-1} range. The circular dichroism spectra were recorded on a JASCO J-810 Spectropolarimeter with KBr pellets. Powder XRD patterns were collected on a D/MAX-3C diffractometer using graphite-mono-chromatized CuKa radiation (λ = 1.5406Å). Variable temperature magnetic susceptibility measurements were carried out in the temperature range of 2–300 K with a Quantum Design MPMS-XL5 SQUID magnetometer. The magnetic data were corrected for the diamagnetic contribution of the sample holder and the diamagnetic contribution of the sample by using Pascal constants. Thermogravimetric analyses (TG) were performed using a Mettler TGA/SDTA851 thermal analyzer under N_2 atmosphere with a heating rate of 10 ℃ min^{-1} in the temperature region of 25–500 ℃. The chemical analysis was carried out using inductively coupled plasma (ICP) methods on an ESCALAB2000 analyzer.

Synthesis of $\{[Zn(en)_2]_2V_{15}O_{36}Cl\}[Zn(en)_2(H_2O)]_2 \cdot 3H_2O$ (1)

A mixture of NH_4VO_3 (0.1189 g), $Zn(CH_3COO)_2$ (0.2774 g), ethylenediamine (en, 0.25 mL) HCl (3 mol· L^{-1}, 0.1 mL) and water (1.0 mL) was stirred for 0.2 h, then final mixture was sealed in a 25 mL Teflon-lined autoclave and heated at 110 °C for 7 days. After cooling to room temperature slowly, pink-block crystals were isolated. The crystals were filtered and dried at room temperature (57 % yield based on NH_4VO_3). Anal. Calc for $C_{16}H_{74}ClN_{16}O_{41}V_{15}Zn_4$ for **1**: C, 8.70; H, 3.38; N, 10.15. Found. C, 8.81; H, 3.37; N, 10.26. ICP analysis shows that the molar ratio of Cl : V : Zn is 0.95 : 15.03 : 3.98, consistent with the stoichiometry.

Crystal Structure Determination

Single-crystal X-ray diffraction data for **1** were recorded on a Rigaku Mercury CCD diffractometer using a ω-scan method with graphite monochromated Mo Kα radiation (λ = 0.71073 Å) at 296(2) K to a maximum 2θ value (53.00 °). Absorption corrections were applied using multi-scan technique. The structure of **1** was solved by Direct Method of SHELXS-97 and refined by full-matrix least-squares techniques using the SHELXL-97 program. Non-hydrogen atoms were refined with anisotropic temperature parameters. The H atoms bonded to C and N atoms were positioned with idealized geometry and refined with fixed isotropic displacement parameters. No H atoms associated with water molecules were located from the difference Fourier map. O1w atom was disordered over two positions with occupation factors of 0.15/0.85. The O3w and O4w have occupancy of 0.5. The one water was not all located because of the serious disorder problems. The unlocated water molecule contribution to the scattering factors has been taken into account with PLATON/SQUEEZE. After applying the SQUEEZE option, the wR2 values decline significantly from 0.1583 to 0.1483. Relevant crystal and collection data parameters and refinement results can be found in Table S1. Additional details of crystal data in CIF format can be found in the Supporting Information.

Table S1 Crystallographic data for **1**.

	1
formula	$C_{16}H_{74}ClN_{16}O_{41}V_{15}Zn_4$
Fw	2207.94
crystal system	Orthorhombic
space group	$P2_12_12_1$
a, Å	12.876(3)
b, Å	18.938(4)
c, Å	28.202(6)
V, Å^3	6877(3)
Z	4

T, K	296(2)
Calcd density,Mg.m^{-3}	2.108
abs coeff, mm^{-1}	3.429
F(000)	4296
2θ(max), deg	53.00
Total reflns collected	44166
Unique reflns	14255
No. of param	848
*R*1[*I*>2σ(*I*)]	0.0495
*wR*2(all data)	0.1483
Absolute structure parameter	0.045(17)

Table S2. Selected Bond Lengths (Å), Bond Valences (v.u.) and Angles (deg) for **1**.

bonds		v^a	bonds		v^a
V1-O28	1.609(5)	1.60	V2-O5	1.618(5)	1.56
V1-O12	1.828(5)	0.88	V2-O12	1.810(5)	0.93
V1-O3	1.921(5)	0.69	V2-O32	1.923(5)	0.68
V1-O30	1.929(5)	0.68	V2-O35	1.924(4)	0.68
V1-O31	2.021(5)	0.53	V2-O7	2.003(5)	0.55
	sum	4.38		sum	4.40
V3-O20	1.623(5)	1.54	V4-O13	1.620(4)	1.55
V3-O23	1.818(5)	0.91	V4-O35	1.952(5)	0.63
V3-O16	1.905(4)	0.72	V4-O34	1.964(5)	0.61
V3-O8	1.917(5)	0.69	V4-O19	1.966(4)	0.61
V3-O6	2.039(5)	0.50	V4-O30	1.970(4)	0.60
	sum	4.36		sum	4.00
V5-O2	1.612(5)	1.58	V6-O18	1.608(5)	1.60
V5-O26	1.804(5)	0.95	V6-O3	1.963(5)	0.61
V5-O34	1.914(4)	0.70	V6-O25	1.972(5)	0.60
V5-O36	1.920(4)	0.69	V6-O32	1.992(5)	0.57
V5-O33	2.024(5)	0.52	V6-O8	1.994(5)	0.56
	sum	4.20		sum	3.94
V7-O10	1.613(5)	1.58	V8-O4	1.634(5)	1.49
V7-O27	1.918(5)	0.69	V8-O22	1.880(5)	0.77
V7-O7	1.926(5)	0.68	V8-O7	1.885(5)	0.76
V7-O35	1.936(5)	0.66	V8-O32	1.931(5)	0.67
V7-O19	1.956(4)	0.63	V8-O25	1.948(5)	0.64
	sum	4.24		sum	4.33
V9-O17	1.616(5)	1.57	V10-O14	1.626(4)	1.53
V9-O23	1.819(5)	0.90	V10-O26	1.827(5)	0.89

V9-O9	1.895(5)	0.74	V10-O21	1.900(4)	0.73
V9-O25	1.901(5)	0.73	V10-O19	1.929(4)	0.67
V9-O22	2.037(5)	0.50	V10-O27	2.015(5)	0.53
	sum	4.44		sum	4.35
V11-O29	1.604(5)	1.62	V12-O24	1.607(5)	1.61
V11-O31	1.881(5)	0.78	V12-O36	1.963(4)	0.61
V11-O33	1.907(5)	0.76	V12-O9	1.964(5)	0.61
V11-O30	1.932(5)	0.67	V12-O16	1.972(5)	0.60
V11-O34	1.934(4)	0.66	V12-O21	1.977(5)	0.59
	sum	4.49		sum	4.02
V13-O15	1.623(5)	1.54	V14-O1	1.627(5)	1.52
V13-O31	1.913(5)	0.70	V14-O33	1.900(5)	0.73
V13-O6	1.917(5)	0.69	V14-O6	1.903(5)	0.72
V13-O8	1.934(5)	0.66	V14-O36	1.936(4)	0.66
V13-O3	1.938(5)	0.66	V14-O16	1.944(5)	0.65
	sum	4.25			4.28
V15-O11	1.617(5)	1.56			
V15-O27	1.877(5)	0.78			
V15-O22	1.883(5)	0.76			
V15-O9	1.940(5)	0.65			
V15-O21	1.941(4)	0.65			
	sum	4.40			

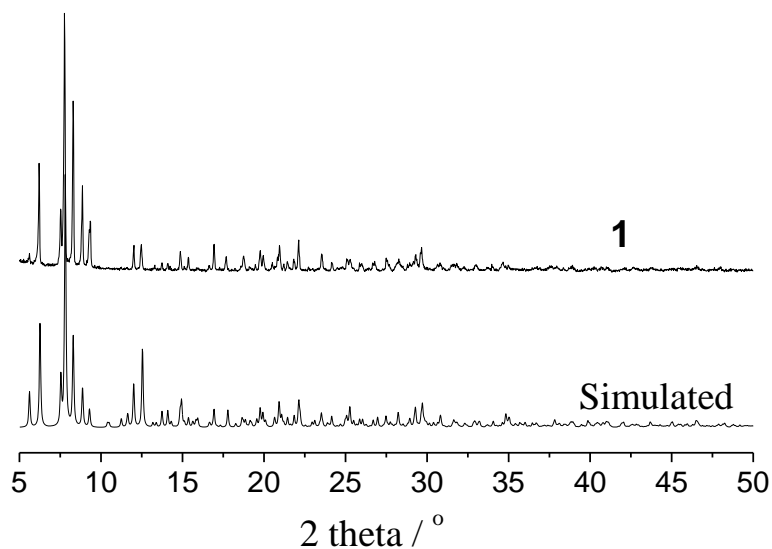[a]Bond valences and their sums calculated using parameters.

Fig. S1 Simulated and experimental powder XRD patterns of **1**.

The experimental peak positions are in agreement with simulated XRD pattern, indicating the phase purity of **1**. The difference in reflection intensity between experimental and simulated XRD

patterns is probably due to the preferred orientation effect of the powder sample during collection of the experimental XRD data.
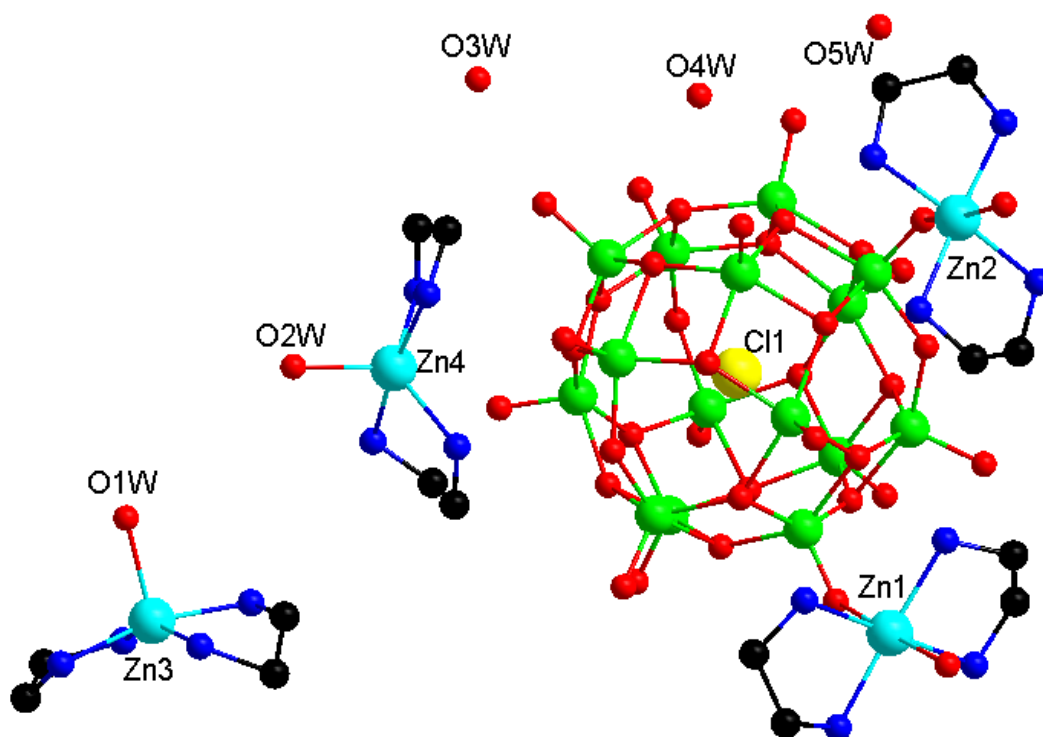

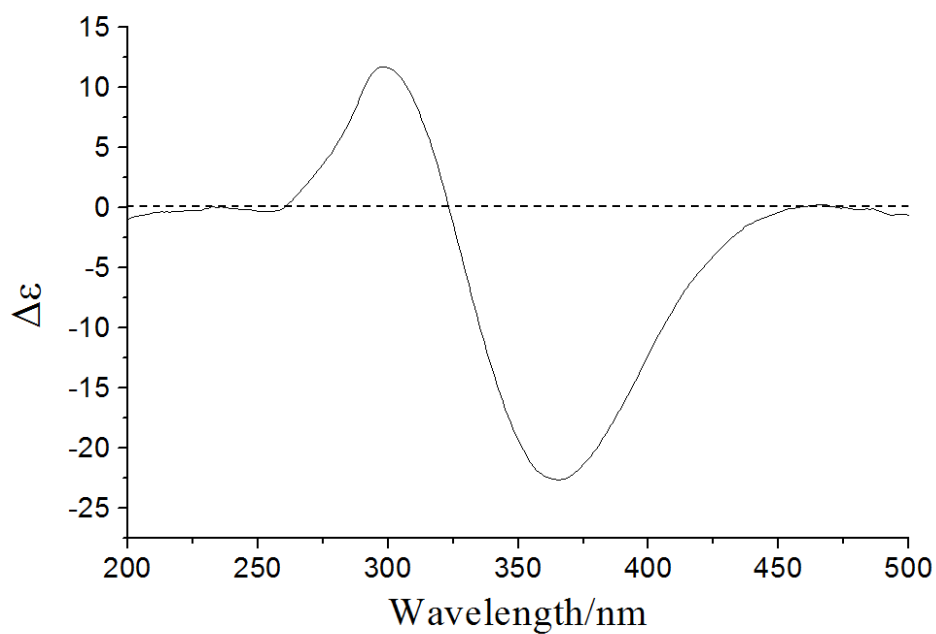Fig. S2 The asymmetric unit of **1**. All H atoms are omitted for clarity.

Figure S3. CD spectrum of **1** (only very few exiguous crystals were used as the measured samples).
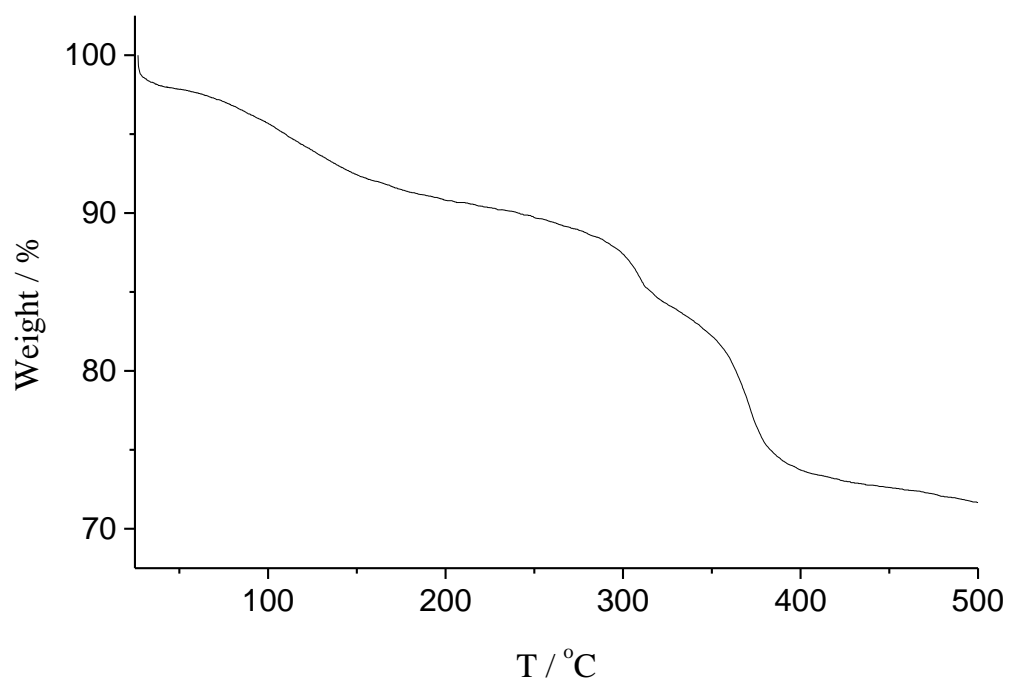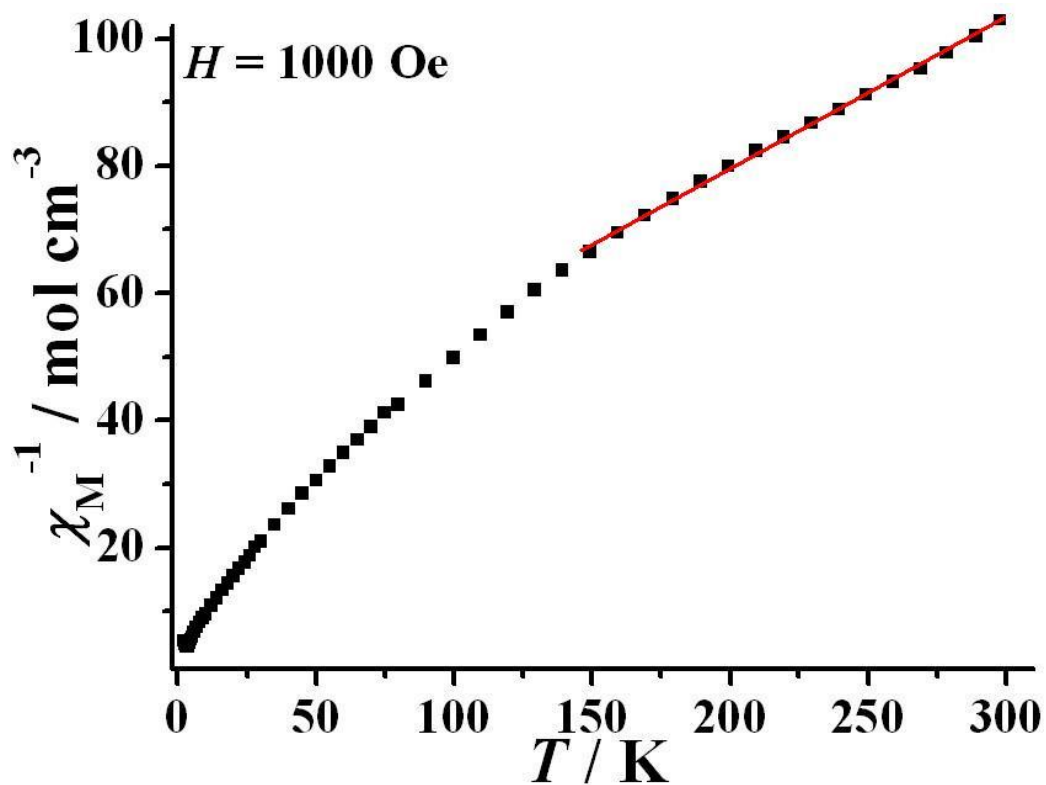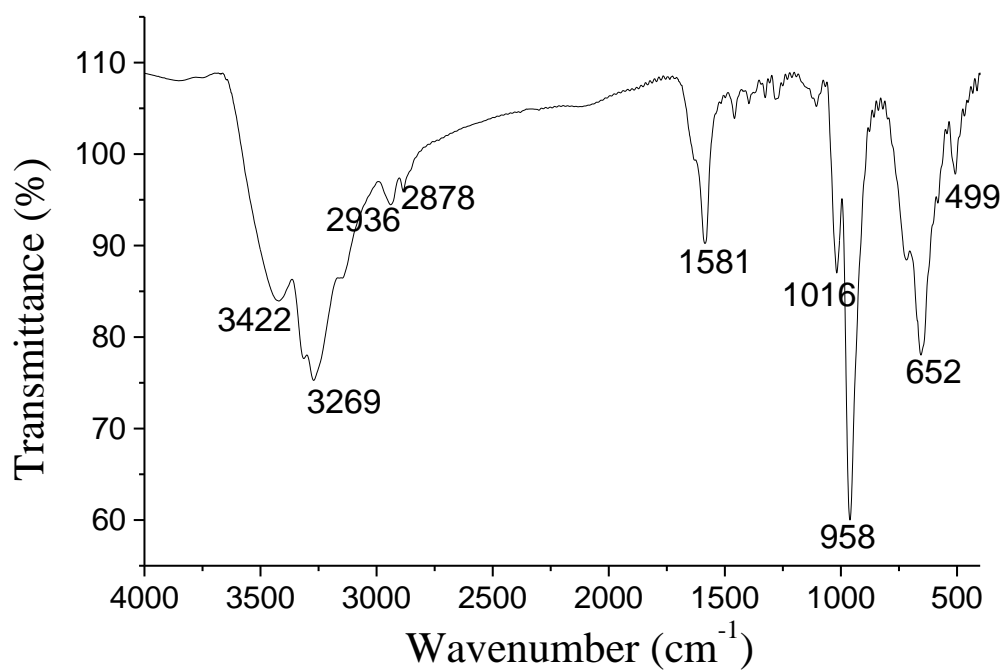
Fig. S4. TG curve of **1**.

Fig. S5 The plot of χ_M^{-1} versus T for **1**.

Fig. S6 IR spectrum of **1**.